Strength And Fracture Behavior of Pipes With Circumferentially Orientated Cracks Under Monotonic Bending Loading

W. Stoppler, D. Sturm, J. Schiedermaier, K. Hippelein
Universität Stuttgart, Stuttgart, FRG

Abstract

Pipes with the dimensions of the main coolant piping system of a pressurized water reactor (PWR) weakened by circumferential flaws and loaded by internal pressure as well as an external bending moment were tested to define the critical flaw length under service and upset conditions.

Introduction

Design, construction and service of a primary cooling system of German Light-Water-Power-Plants is based on the concept of basis safety, which is incorporated into the KTA-rules 3201.1 and 3201.2 /1/. A catastrophic failure of a pressurized component can be excluded observing these rules. The aim of the research project "Phenomenological Vessel Burst Test", /2, 3, 4, 5/ which is sponsored within the scope of the reactor safety research program, Fig. 1, of the Federal Ministery for Research and Technology (BMFT) is to prove the integrity of the piping loaded under all possible in service and emergency conditions. In accordance with the KTA-rules, emergency conditions such as earthquake, waterhammer or airplane crash can cause stresses higher than the yield strength. The design of the component as well as the used material have to be able to reduce stress peaks by local yielding.

Objectives

Pipes with an O.D.=800 mm and a wall thickness of 47 mm, which are the main dimensions of the primary cooling piping of a German 1300 MW_e PWR, were investigated under service conditions referring to internal pressure (~15 MPa) and temperature (up to 300 °C). Aditionally, a monotonic increasing outer bending moment was applied. Most of the pipes were weakened by machined cracks in circumferential direction. Fig. 2 shows the investigated parametric field regarding the kind of flaws, inner and outer surface notches resp. through-wall cracks (slits), as well as the flaw dimensions, length and depth. To investigate also the influence of toughness, the pipes were fabricated of two kinds of fine grain ferritic steels with nearly the same strenght properties (300 °C) such as ultimate strenght R_m ~ 605 MPa and a yield strenght $R_{p0,2}$ ~ 428 MPa. One material, 20 MnMoNi 5 5, had a high upper shelf impact energy of > 150 J (HUSE), and the other, NiMoCr-melt, had a low upper shelf impact energy of ~ 50 J (LUSE).

Methods

The 5 m long pipes were mounted into a four-point bending device with a capacity of 14 MNm. The bending moment could be applied by means of an actuator, positioned above the center line of the pipe, Fig. 3. To achieve a system which is as soft as possible air was used as pressure medium for the actuator and the pipe. Electric power heat pads were wrapped around the pipe to obtain the elevated temperature.

Results

In Table 1 the results are listed of all performed tests. First of all, the load (bending moment)-strain behavior of the unweakened pipe was determined, Fig. 4. A bending moment M_{bF} = 9,3 MNm was found at the end of the elastic range and at the point of an equivalent plastic strain of 0,2 % a bending moment $M_{b0,2pl}$ = 11,5 MNm. As shown in the lower part of Fig. 4 the experimentally determined bending moment-strain curve corresponds very well with a calculated one /6/, taking into account the deviation of material properties and dimensions.

The load bearing capacity of pipes, weakened by circumferentially orientated slits are plotted for both materials as scatterband in Fig. 5. These curves represent also the leak-before break curves, which separates the area of "leakage" from that of the "catastrophic failure". It becomes obvious, that the load bearing capacity is significantly influenced by the thoughness of the material. The critical slitlength of pipes made of the HUSE-material amounts more than twice the quantity achieved for the pipes made of the LUSE-material. From the path of the curves it can also be seen that the critical length of a defect can become relatively small when increasing the external bending moment. Following KTA-rules for level D (emergency and upset conditions), a stress limitation of 3 Sm is given. This means, that a bending moment of 10 MNm has to be considered if the specified material properties were used for calculation or a moment of 11,5 MNm if the actual ones were used. Both figures are within the range of $M_{b0,2pl}$ of the unweakened pipe. The corresponding critical slit length is given by Fig. 5 to 390 mm (56°) resp. 240 mm (35°) for pipes of HUSE-material. These values shrink to 180 mm (26°) resp. 100 mm (15°) in pipes of LUSE-materials. The last value stands for the worst case consideration and it has to be kept in mind, that this value is at least 3 times greater compared with the permissible lenght of a surface defect which according to /7/ is approx. 30 mm. The results of the experiments with pipes weakened by circumferential surface-flaws show also a determinative influence of the material toughness to the load bearing capacity, Fig. 6 and 7.

The experimentally determined failure moments were compared with calculated ones, Figs. 8 and 9, by means of two mainly used engineering methods /5, 9, 10/, Table 2. Regarding the investigated dimensions of the pipes as well as the materials, the following statements could be made:

- The "Moment Method" underestimates the load bearing capacity of the HUSE-pipes by roughly 30 % and
- overestimates by roughly 20 % the load bearing capacity of the LUSE-pipes.

- The "Plastic collapse method" delivers values which are in the range of the experimetally determined, if the failure moment lies above the yield moment $M_{bF} > 9$ MNm, Fig. 10. Otherwise, a higher failure moment is calculated than received by the experiment.

Conclusions

The experimentally determined critical slit length for main cooling piping of a PWR is much greater than the detectable one by means of NDT even if a bending moment under emergency conditions is applied and the toughness of the material is in the EOL-status. The leak-before-break criterion could be proved. The toughness has a significant influence on the load bearing capacity and the failure mode. The engineering calculation methods need more improvement to take into account material thoughness.

Literature

/1/ Sicherheitstechnische Regeln des kerntechnischen Ausschusses, KTA 3201.1 und KTA 3201.2.
Carl Heymanns Verlag KG, Köln

/2/ Forschungsvorhaben "Phänomenologische Behälterberstversuche" 150279, Abschlußbericht Phase I, Juli 1985, MPA Stuttgart.

/3/ **Kussmaul, K., D. Sturm, W. Stoppler and D. Müller-Ecker:** Experimental Investigation on the Crack Opening Behaviour of Cylindrical Vessels under Light Water Reactor Service Conditions. Reliability and Safety of Pressure Components. The American Society of Mechanical Engineers. New York, N.Y., 1982, PVP-Vol. 62, pp. 97/134.

/4/ **Sturm, D. et. al.:** Fracture Initation and Fracture Opening under Light Water Reactor Conditions.
Nuclear Engineering and Design, Vol. 72 (1982) No. 1, pp. 81/95.

/5/ **Stoppler W., J. Schiedermaier, K. Hippelein, D. Sturm and S. Shen:** Crack Behaviour of Pipes under Internal Pressure and Simultaneous External Bending Moment. Nuclear Engineering and Design, March 1989

/6/ **Wellinger, K. und H. Dietmann:** Festigkeitsberechnung
A. Kröner Verlag Stuttgart, 1969.

/7/ **Bartholomé, G.:** Anwendung der Bruchmechanik für kerntechnische Anlagen. Haus der Technik, Tagung Nr. T-30-908-111-6, 06.11.1986, Essen.

/9/ **Kanninen, M.F., et. al.:** Instability Predictions on Circumferentially Cracked Type 304 Stainless Steel Pipes under Dynamic Loading.
NP-2347, Vol. 1, Research Project T118-2, Final Report (April 1982).

/10/ **Shibata, K., Y. Yasuda, K. Omizawa und S. Miyazono:** Progress of Ductile Pipe Fracture Test Program at JAERI,
LBB Seminar, Tokyo, 1987.

Test Identi-fication	Dimen-sions mm	Type	Crack Angle Degree	Depth mm	Temp. °C	Internal Pressure (Air) MPa	Max. Bending Moment Experim. M_{bexp} kNm	Bending Moment Slit macro-scopic Elongation kNm	Ligament Start of Break-Through kNm	Ligament End of Break-Through kNm	Comments
BVZ 090		0	-	-	20	15,2	12.110	-	-	-	not achieved M_{bmax}
BVZ 161	Outer	S	20	47,2	130	0,0	13.910	13.910	-	-	Instable crack 240 degree
BVZ 091	Diam-	S	60	47,2	20	0,0	9.650	9.200	-	-	Ceased at 170 grd
BVZ 100	eter	S	60	47,2	5	15,0	8.970	5.000	-	-	Ceased at 180 grd
BVZ 160	800	A	20	26,0	233	14,6	13.110	-	13.090	13.090	Leakage
BVZ 110		A	60	39,4	220	13,4	7.050	-	7.050	7.050	Leakage
BVZ 120	Wall	A	60	20,0	195	13,3	11.030	-	10.500	9.800	Leakage
BVZ 130	thick-	I	60	20,0	235	15,2	11.300	-	9.300	8.400	Leakage
BVZ 150	ness	A	90	20,0	267	15,7	9.300	-	7.690	6.390	Rupture
BVZ 140	47,2	A	120	20,0	248	15,2	8.300	-	6.630	4.840	Leakage
BVS 090	Length	0	-	-	250	14,8	11.500	-	-	-	not achieved M_{bmax}
BVS 060	5000	S	60	47,2	140	15,6	5.510	5.200	-	-	Instable crack 240 degree
BVS 110		A	20	36,0	247	15,3	8.500	-	8.500	8.500	Leakage
BVS 102		A	20	20,0	235	15,1	11.240	-	10.700	10.700	Rupture
BVS 070		A	60	20,0	232	16,0	6.600	-	6.600	6.100	Leakage
BVS 080		A	120	20,0	253	14,8	5.550	-	5.200	5.050	Rupture

BVZ: Material 20 MnMoNi 55 (Upper Shelf Impact Energy A_v > 150 J)
BVS: NiMoCr-melt (Upper Shelf Impact Energy A_v ~ 50 J)

Type of Crack A: Outer Surface Crack
I: Inner Surface Crack
O: Without Crack
S: Slit

Table 1: Summary of Test Results

Calculation of the Failure Moment of Pipes Exposed to Internal Pressure and External Bending				
	Circumferential Flaw		Through-Wall Crack	
Theory	Bernoulli "Moment"-Method	Net Section Collapse	Bernoulli "Moment"-Method	Net Section Collapse
Criterion	Tensile Strength	Flow Stress	Tensile Strength	Flow Stress
Formula M_b =	$\frac{I_t}{a}(R_m - \frac{A_w}{A_q - A_f} p_i) - (\hat{y} + b) A_w p_i$	$2\sigma_f r^2 \cdot s(2\sin\beta - f\sin\alpha)$ für $\beta + \alpha > \pi$ $2\sigma_f r^2 s[2(1-f)\sin\beta' + f\sin\alpha]$	$\frac{I_t}{a}(R_m - \frac{A_0}{A_q - A_f} p_i) - \hat{y} A_0 p_i$	$2\sigma_f r^2 s(2\sin\beta - \sin\alpha)$
Factors	$I_t = I_x - \hat{y}^2(A_q - A_f) - (A_f + \frac{\sin 2\alpha}{8}(D^2 - d^2))\frac{D^2 + d^2}{16}$ $I_x = \frac{\pi}{64}(d_a^4 - d_i^4)$ $\hat{y} = \frac{1}{12}\frac{\sin\alpha(D^3 - d^3)}{A_q - A_f}$ $A_q = \frac{\pi}{4}(d_a^2 - d_i^2)$ $A_0 = \frac{\pi}{4} d_i^2$ Inner Surface Notch $D = d_1$, $d = d_i$, $a = \hat{y} + \frac{d_a}{2}$ $b = \frac{1}{12}\frac{\sin\alpha(d_1^3 - d_i^3)}{A_0 + A_f}$ $A_w = A_0 + A_f$ $A_f = \frac{1}{4}\text{arc}\,\alpha(d_1^2 - d_i^2)$ External Surface Notch $D = d_a$, $d = d_1$, $b = 0$ $A_f = \frac{1}{4}\text{arc}\,\alpha(d_a^2 - d_1^2)$, $A_w = A_0$ $a = \hat{y} + \frac{d_1}{2}$ For $d_a\cos\alpha < d_1$ $a = \hat{y} + \frac{d_a}{2}\cos\alpha$ For $d_a\cos\alpha \geq d_1$	$\beta = \frac{\pi - f\alpha}{2} - \frac{\pi r p_i}{4 s \sigma_f}$ $\beta' = \pi + \frac{1}{1-f}(\frac{f\alpha - \pi}{2} - \frac{\pi r p_i}{4 s \sigma_f})$ σ_f z.B. $\frac{1}{2}(R_m + R_{p0,2})$ $\sigma_f = R_{eH}$ bzw. $R_{p0,2}$ $f = \frac{t_1}{s}$ $r = \frac{d_a - s}{2}$	$I_t = I_x - \hat{y}^2(A_q - A_f) - (A_f + \frac{\sin 2\alpha}{8}(d_a^2 - d_i^2))\frac{d_a^2 + d_i^2}{16}$ $I_x = \frac{\pi}{64}(d_a^4 - d_i^4)$ $\hat{y} = \frac{1}{12}\frac{\sin\alpha(d_a^3 - d_i^3)}{A_q - A_f}$ $a = \hat{y} + \frac{d_a}{2}\cos\alpha$ für $\alpha \leq 90°$ $a = \hat{y} + \frac{d_i}{2}\cos\alpha$ für $\alpha > 90°$ $A_0 = \frac{\pi}{4} d_i^2$, $A_q = \frac{\pi}{4}(d_a^2 - d_i^2)$ $A_f = \frac{1}{4}\text{arc}\,\alpha(d_a^2 - d_i^2)$	$\beta = \frac{\pi - \alpha}{2} - \frac{\pi r p_i}{4 s \sigma_f}$ σ_f z.B. $\frac{1}{2}(R_m + R_{p0,2})$ $\sigma_f = R_{eH}$ bzw. $R_{p0,2}$ $r = \frac{d_a - s}{2}$

Stress Distribution

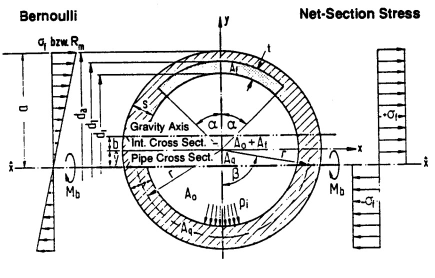

Stress Distribution

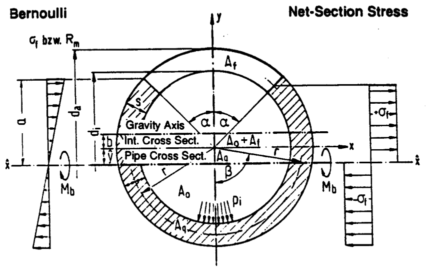

Table 2: Engineering Approaches

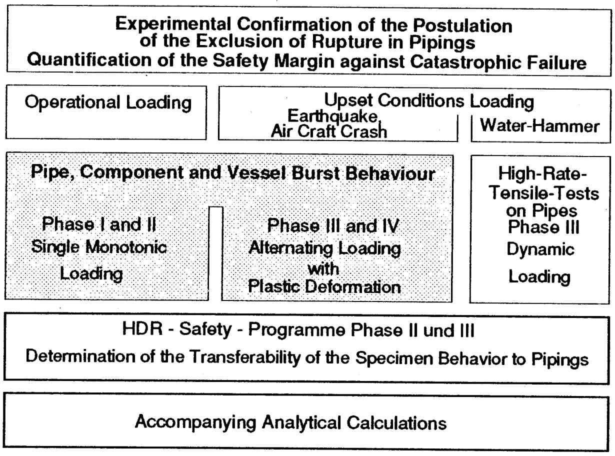

Fig. 1: Research Projects within the Scope of Reactor Safety

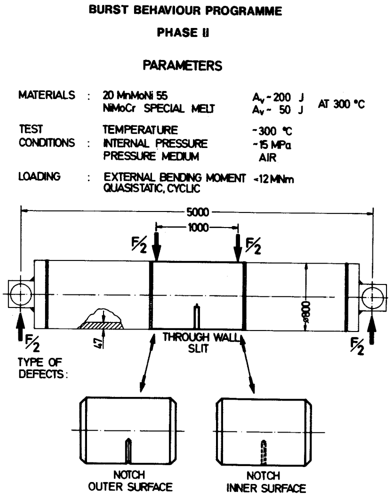

BURST BEHAVIOUR PROGRAMME

PHASE II

PARAMETERS

MATERIALS	:	20 MnMoNi 55	A_v ~ 200 J	AT 300 °C
		NiMoCr SPECIAL MELT	A_v ~ 50 J	
TEST CONDITIONS	:	TEMPERATURE	~300 °C	
		INTERNAL PRESSURE	~15 MPa	
		PRESSURE MEDIUM	AIR	
LOADING	:	EXTERNAL BENDING MOMENT QUASISTATIC, CYCLIC	~12 MNm	

Fig. 2: Parametric Field

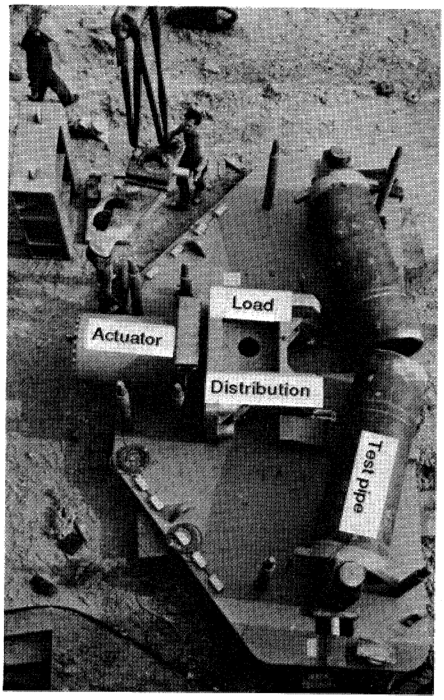

Fig. 3: 14 MNm Four-Point Bending Device

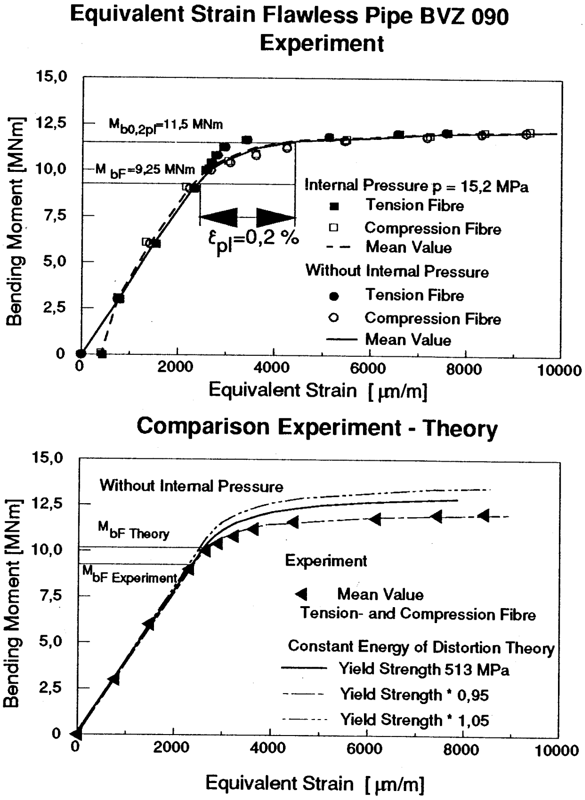

Fig. 4: Load - Strain Behavior of an Unweakened Pipe

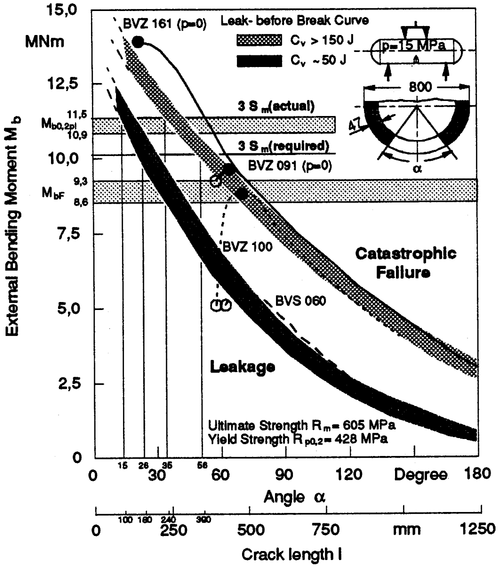

Fig. 5: Leak- before Break Curves

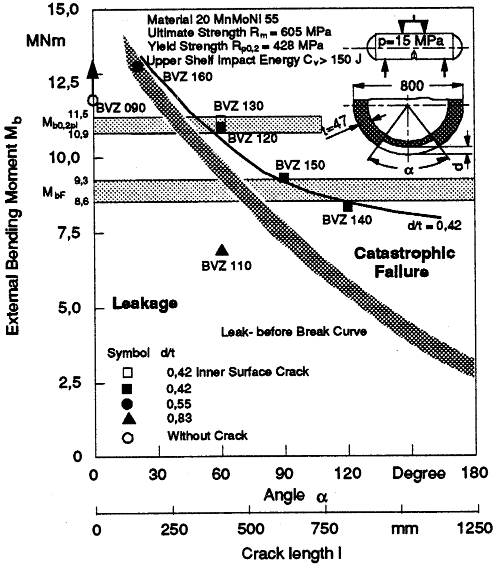

Fig. 6: Load Bearing Capacity of HUSE-Pipes

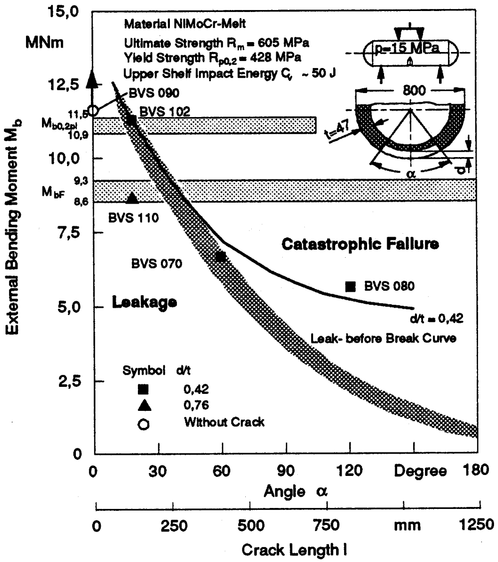

Fig. 7: Load Bearing Capacity of LUSE-Pipes

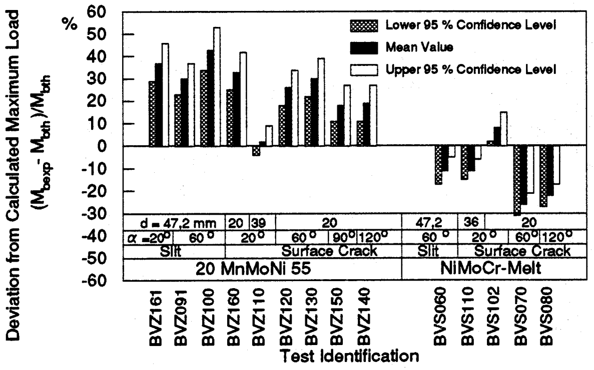

Fig. 8: Comparison Experiment with Engineering Approach "Moment Method"

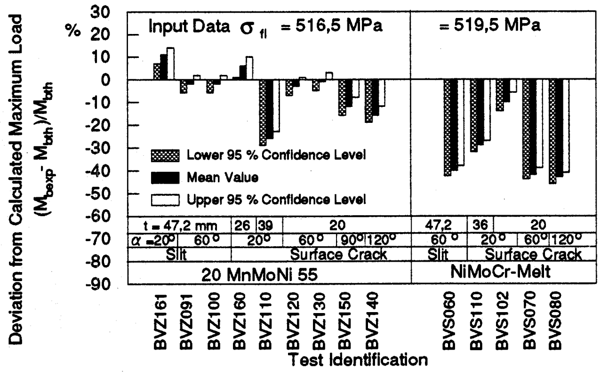

Fig. 9: Comparison Experiment with "Net Section Collapse" - Method

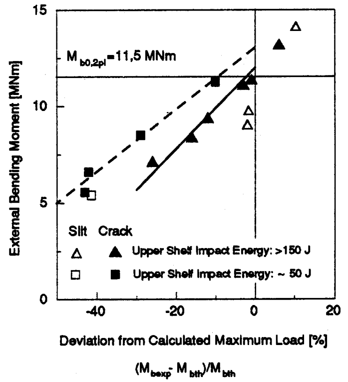

Fig. 10: "Net Section Collapse"